



PID CONTROLLER APPLIED TO AN UNMANNED AERIAL VEHICLE

Diego F. Sendoya-Losada and Jesús D. Quintero-Polanco

Department of Electronic Engineering, Faculty of Engineering, Surcolombiana University, Neiva, Huila, Colombia

E-Mail: diego.sendoya@usco.edu.co

ABSTRACT

Unmanned Aerial Vehicles (UAV) has gained interest from the academic community worldwide, especially due to their numerous applications in civil and military applications. The advances in sensor technology, communication and microcontrollers have allowed the research community to develop such applications. The first part of this contribution is focused on the architecture of such a system, while in the second part of the paper the modelling, identification and controller for the yaw movement of the helicopter is presented. The obtained controller was tested in real-life experiments with very good results.

Keywords: identification, modeling, PID Control, UAV.

1. INTRODUCTION

Helicopters pose special abilities which are not encountered in any other flying machine. Some of these special abilities are: hovering, vertical takeoff-landing, low-speed cruise, pirouette, etc.; which come together with a manifold of challenges. The helicopter dynamics can be characterized by a MIMO (Multi Input Multi Output) strongly coupled system with nonlinearity and intrinsic instability [8]. Hitherto, the research towards modelling and control of such a UAV (Unmanned Aerial Vehicle) system has known an increased interest from the academic community, given the great number of papers and projects concerned with this topic. This major interest is due to the various applications of UAVs, both for military and civil purposes. A comprehensive list of civil applications is presented in [12], e.g. scientific missions, emergency missions, surveillance missions, and industrial applications.

The application presented in this paper is a UAV platform based on a commercially available coaxial helicopter which is shown in Figure-1. The final purpose of this research project is to achieve autonomous flight conditions suitable for surveillance in narrow spaces, e.g. inside a commercial center [3].

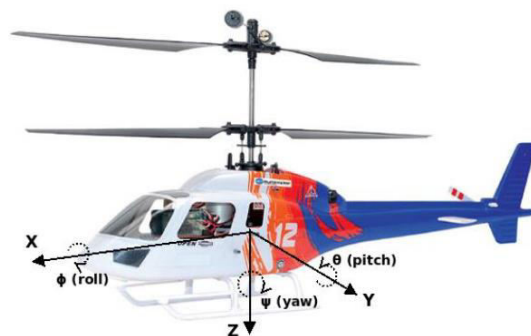


Figure-1. Coaxial helicopter.

In this contribution, the first steps towards complete modelling, identification and control of coaxial

helicopter are presented. Initially, a SISO configuration is proposed based on a simplified model, which enables control on one of the three axes - the Z axis (yaw). The identification is achieved using a revised form of the classical transfer function analyzer (TFA) algorithm; namely the Chirp-TFA [5]. Once the model is available, the design of the controller can be performed based on the desired specifications of the closed loop performance. For this purpose, the FR tool (Frequency Response Toolbox) for Matlab environment has been employed [7].

The paper is structured as follows: initially the structure of the UAV system is presented (hardware and software); then a model for the yaw movement of a miniature coaxial helicopter is proposed; next section deals with the identification of the yaw movements; then the control strategy is presented; and in the last section the paper is summarized and some further research is proposed.

2. MATERIALS AND METHODS

2.1 UAV System

The use of a coaxial helicopter for a UAV system development has been reported in several papers [3, 4, 13, 14]. This type of aircraft is easier to control than the single rotor helicopter and the power is used more efficiently due to the absence of a tail rotor.

The UAV system consists of: 1) the aircraft to be controlled; 2) an on-board IMU (Inertial Measurement Unit) with sensors to determine the attitude of the aircraft; 3) bidirectional wireless communication; and 4) a ground-based computer in which the controller is implemented. A block representation of the hardware system is shown in Figure-2. The arrows that interconnect the components indicate how data is transmitted through the system. Solid lines represent wired communication while dotted lines represent wireless communication.

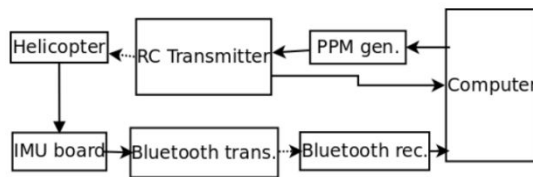


Figure-2. Block scheme of the UAV components.

In general, for automatic control of a process, the controller must be able to send commands to the process and receive information about the output of the process. The communication inside the UAV system can be split in two communication links that connect the helicopter to a computer which runs the control algorithm.

First link is the control link which is used to send the control sequence from the computer to the helicopter. This link consists of two devices: the RC (Radio Control) transmitter and the PPM (Pulse Position Modulation) generator. The RC transmitter is equipped with joysticks which are used for sending the user commands to the helicopter. The device was modified such that it is possible to switch between computer control and manual control using a mechanical switch. The PPM generator is connected on the serial port of the computer and is used in automatic mode to convert the values generated by the computer into a PPM signal. The helicopter has four communication channels: throttle, elevator, rudder and aileron which correspond to the four inputs of the helicopter: altitude control, pitch, yaw and roll. In the current implementation, only the yaw channel is controlled by the computer. The other three movements are controlled and stabilized by the user using the joysticks. In automatic mode the values for throttle, elevator and aileron are read by the computer from the joysticks and then transmitted to the helicopter using the PPM generator and the RC transmitter. In this operation mode, the rudder channel is controlled by the digital controller implemented on the computer.

The second communication link is the feedback link which consists of a Bluetooth transmitter and a Bluetooth receiver. This link makes the connection from the microprocessor which gathers the data from the sensors on the IMU (Inertial Measurement Unit) board and the controller that runs on a computer. The data read from the sensors is organized in frames which are sent through the wireless link to the computer. Bluetooth communication can have a maximum range of 100 meters inside which is enough for our current purposes. Wireless communication is affected by random variable delays when data packets get lost on the way to their destination. For our setup the delays can go up to 40 ms. A simple solution is to consider the previously received data when such a delay occurs.

The helicopter used is Big Lama, manufactured by Esky. It has a coaxial structure with two counter-rotating main rotors and no tail rotor. This structure has the advantage that it is more stable than the classical single

rotor configuration. The main characteristics of the helicopter are presented in Table-1.

Table-1. Physical specifications of the helicopter.

Main rotor diameter	460mm
Weight	410g
Length	510mm
Width	110mm
Height	260mm
Motors	code 370 (2 installed)
Battery	11.1V 800mAh Li-polymer

The sensors are integrated in an Inertial Measurement Unit (IMU) which consists of: a 32-bit microprocessor, 3-axis accelerometer, 3-axis angular rate sensor (gyroscope), a 12-channel GPS receiver, a dynamic pressure sensor, a static pressure sensor, a temperature sensor, a voltage sensor and a current sensor.

The active elements in the UAV system that run a software program are the computer, the PPM generator and the IMU board.

The software on the PPM generator is used for converting the values received by the PIC micro-controller into a time modulated PPM signal, see Figure-3. There are 6 channels modulated in the PPM signal out of which only four are used. The length of every channel can vary between 0.5 ms and 1.6 ms. There is a constant period of 0.4 milliseconds between two consecutive channels during which the output of the signal changes to low. This period is used to differentiate between two consecutive channels.

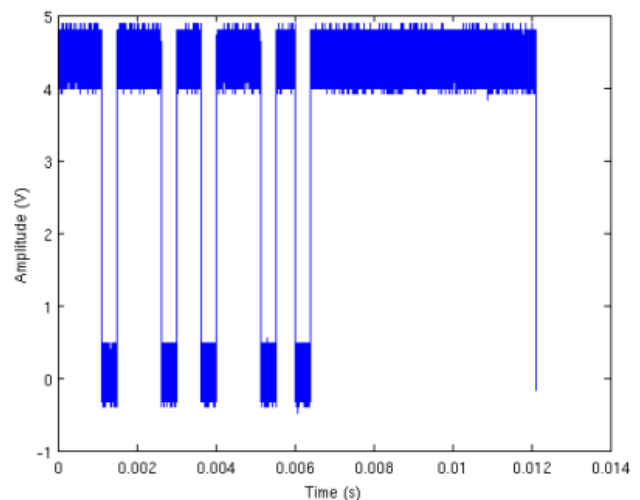


Figure-3. Measured PPM signal.

The block diagrams of the routines used for generating the PPM signal are presented in Figures 4 and 5. The interrupt handler routine in Figure-4 is used for setting the signal high or low for the specified amount of time. Left branch sets the output low for a period of 0.4 ms between two channels and the right branch sets the output high for the time received from the computer. The data



reading routine in Figure-5 waits for the data coming from computer and it stores it at the corresponding location. Data frames sent from the computer to the PPM generator start with a zero byte to signal that data is about to follow and after that the value for each channel. In the case of a transmission error, the controller will recover when it receives the next zero byte - which should not take more than 12 ms. This interval is small enough to maintain the stable functioning of the helicopter.

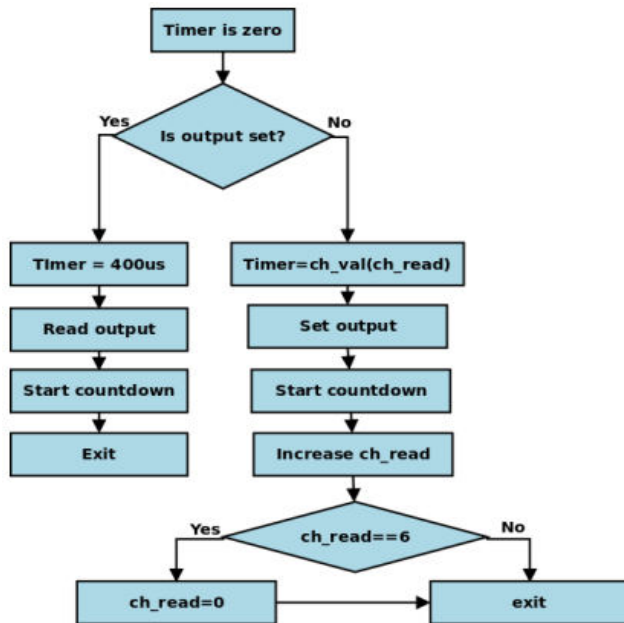


Figure-4. Interrupt handler routine in PPM generation.

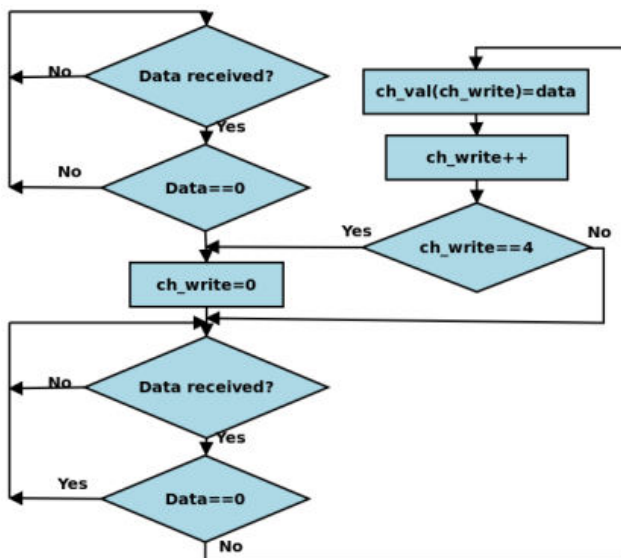


Figure-5. Data reading routine in PPM generation.

The software running on the IMU board continuously reads the data from the sensors and sends it to serial port of the microcontroller. Data read from the sensors is packed into frames of a fixed length of 20 bytes.

The software used for controlling the helicopter runs in real time on a computer and has the purpose to read, store and process the data measured by the sensors, read the pilot's commands, generate commands when the automatic mode is activated. The current version of the control program was written in C programming language and it consists of three threads, see Figure-6.

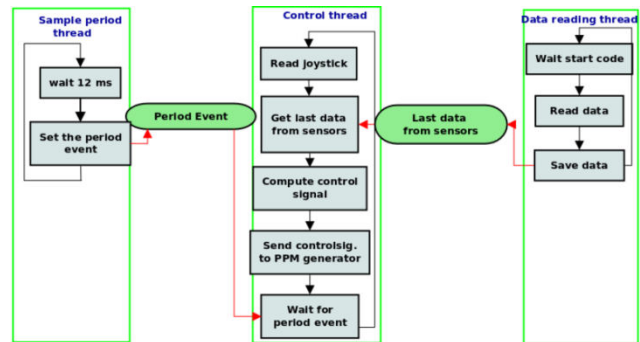


Figure-6. General design of the control program.

The timing thread is used for generating a fixed time interval which represents the sampling period. This thread generates a signal, every 12 ms, which is received by the control thread. The data reading thread continuously reads the data coming from the sensors.

The control thread reads the commands sent by the pilot using the joysticks on the RC transmitter, fetches the last frame of data arrived from the sensors on the helicopter and after that computes and sends the commands to the helicopter. On this latter thread, a two-loop cascade controller is implemented, which computes the control input for the yaw angle. The program sends the control value for the yaw angle (on the Z axis).

2.2 Modeling

In this section an electro-mechanical model of the yaw movement is proposed. The modelling takes into consideration some simplifying conditions such that the obtained model is not too complex to be used for controller design, but still characterizes reasonably well the behavior of the real plant.

The two coaxial counter-rotating rotors are driven by two DC motors. A DC motor can be modelled considering the resistance and the inductance of the coil and the induced backward voltage:

$$u = u_e + Ri + L \frac{di}{dt}$$

where i is the current through the circuit, u is the voltage at the input of the motor, u_e is the voltage induced by the movement of the rotor in the electric field of the permanent magnet, R is the electrical resistance and L is the inductance of the coil.

The mechanical equation for the torque on the shaft can be derived using Newton's second law of



motion, and considering a friction force proportional to the angular rate:

$$\tau = J \frac{d\omega}{dt} + B\omega$$

where τ is the torque generated by the DC motor on its shaft, J is the moment of inertia of the rotating mass, ω is the angular rate of the rotor and B is the viscous friction coefficient. The first term can be neglected if it is considered that the rotation speed of the blades is more or less constant during the flight of the helicopter and due to the fact that the dynamics of the helicopter's body are much slower compared to the dynamics of the rotor blades. After this simplifying assumption, the equation becomes:

$$\tau = B\omega$$

The following equations link the electrical part with the mechanical part:

$$u_e = K_e \omega$$

$$\tau = K_t i$$

where K_e is a constant that links the induced voltage with the angular rate of the rotor and K_t is a constant that links the current flowing through the coils of the motor to the generated mechanical torque. By substituting ω , i and u_e in previous equations and applying the Laplace transform, the following transfer function between torque and input voltage is obtained:

$$\tau(s) = \frac{\frac{K_t}{L}}{s + \frac{R}{L} + \frac{K_e K_t}{BL}} u(s)$$

The coaxial helicopter has two counter-rotating rotors. According to the simplification, the torques generated by the upper and the lower rotors can be expressed as:

$$\tau_{top} = B\omega_{top}$$

$$\tau_{bot} = B\omega_{bot}$$

whereas the two rotors spin in opposite directions. In order to prevent the body of the helicopter from rotating, the two torques must be equal in magnitude. When yaw movement is performed, the rotors should maintain the same lift force, hence the torque generated by one rotor should increase while the torque generated by the other rotor should decrease with the same amount. It is denoted with Γ the torque exerted on the helicopter's body and with $\Delta\tau$ the variation in torque for the two rotors:

$$\Gamma = \tau_{top} - \tau_{bot} = 2\Delta\tau$$

Expressing $\Delta\tau$ according to the transfer function, it can be written:

$$\Gamma(s) = \frac{2 \frac{K_t}{L}}{s + \frac{R}{L} + \frac{K_e K_t}{BL}} \Delta u(s)$$

The above relation directly links the torque of applied on the helicopter's body to the voltage difference between the two DC motors. It is denoted by r the angular rate of the helicopter's body, J_h is the moment of inertia of the body and B_h is the friction coefficient of the body with the air. The equilibrium condition for the body can be written as:

$$\Gamma = J_h \frac{dr}{dt} + B_h r$$

If it is taken into account that the helicopter rotates at low angular speeds (150°/s), it is feasible to ignore the air friction coefficient. In this case, the above relation reduces to:

$$\Gamma = J_h \frac{dr}{dt}$$

From previous equations, it can be obtained:

$$\Gamma(s) = \frac{2 \frac{K_t}{L}}{s + \frac{R}{L} + \frac{K_e K_t}{BL}} \frac{1}{J_h s} \Delta u(s)$$

There is a gyroscope on the helicopter which is used for controlling the yaw movement. The measurements from the gyroscope are introduced into a P controller which can be manually tuned on the helicopter. However, this control loop is sensitive to initialization errors and most of the time the helicopter will have a slow rotational speed on the yaw axis because of improper initialization of the offset for the controller. The gain of the controller is denoted by K , hence one obtains:

$$H_{yaw} = \frac{\frac{2K_t}{L J_h}}{s^2 + \left(\frac{R}{L} + \frac{K_e K_t}{BL}\right)s + \frac{2KK_t}{L J_h}}$$

The terms of this transfer function can be determined if one is able to measure the physical values of the coefficients. In practice is quite difficult to determine these constants given the fact that we are using a commercially available helicopter. In this case, a "black-box" identification may be a good solution. The transfer function determined by physical modeling the yaw dynamics is used as a guideline for the result of the process of identification.



3. RESULTS AND DISCUSSIONS

3.1 Identification

The process to be controlled is a MIMO system with 4 inputs (elevator, aileron, rudder and throttle) and four outputs (roll, pitch and yaw angles and altitude), see Figure-7. The aileron and elevator control the roll and pitch angles by deflecting the swash-plate connected to the lower rotor. The rudder controls the difference of rotational speed of the two rotors producing a torque on the helicopter's body which changes the yaw angle. The throttle controls the power to the two rotors with a direct influence on the altitude of the aircraft.

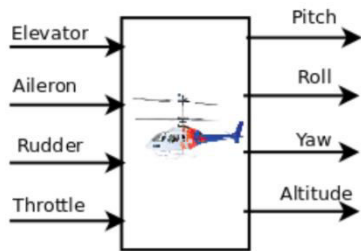


Figure-7. MIMO helicopter system.

Ignoring the coupling between the inputs and the outputs of the system, the system can be approximated using 4 simple SISO transfer functions. This assumption is valid especially for the yaw angle, which is very little influenced by the other three inputs. This angle can be measured with some degree of accuracy using the gyroscope that measures the angular rate around the Z axis. By using this simplified model, the altitude and attitude of the helicopter can be regulated with PID controllers, which has advantages a simpler structure, straightforward design process, and low computational load [2, 9].

3.1.1. Identification Using CIPHER

As a first approach to identifying the yaw transfer function, a software package designed for helicopter identification was used. This software package is called CIPHER (Comprehensive Identification from Frequency Responses) [16] and it was developed by the US Army and the University of California. CIPHER can be successfully used for the identification of miniature helicopters as it was reported in [1, 6, 10, 11].

The recommended input when using CIPHER is a sine sweep signal that covers the whole frequency range of interest [16]. A sine sweep is a sinusoidal signal in which the frequency varies with time. The logarithmic variation of the frequency is given by the following formula:

$$f_i(t) = f_1 \left(\frac{f_2}{f_1} \right)^{\frac{t}{T_f}}$$

where $f_i(t)$ is the instantaneous frequency at moment t , f_1 is the start frequency and f_2 is the instantaneous frequency at the final time T_f . In order to compensate for the transitory regime of the plant, two constant amplitude regions with zero amplitude were added at the beginning and at the end of the input signal.

The frequency range chosen to perform the identification experiment was from 1 Hz to 5 Hz. The amplitude of the input signal varies between ± 0.2 . This value is directly proportional to the difference in speed between the two counter-rotating rotors of the coaxial helicopter. The chirp signal from Figure-8 was applied to the process. The measured response is also shown in Figure-8.

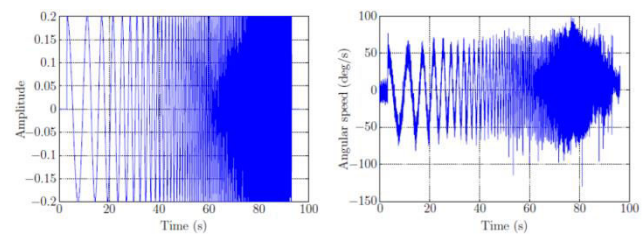


Figure-8. Chirp experiment: input (left) and output (right) signals.

After recording the experimental data, resampling by linear interpolation was performed. Resampling is necessary because the program does not run under a real-time operating system with hard real-time constraints. As a consequence of this, the sampling time may vary within 1-2 ms.

The second step performed for data pre-processing was filtering. The main source of noise in the system comes from the vibrations of the rotors, see Figure-9. The noise has its maximum power between 25 and 30 Hz. In order to reduce this effect, a Butterworth filter with the cut-off frequency of 6 Hz was used.

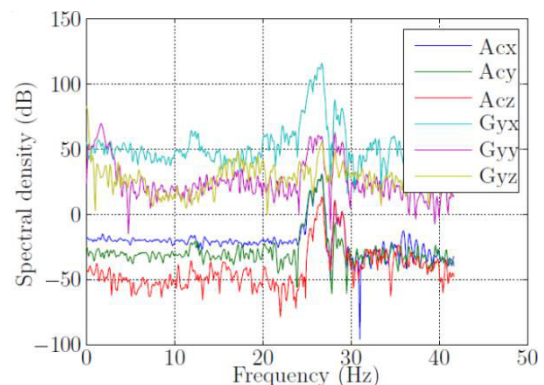


Figure-9. Spectral analysis of the noise caused by vibrations from the rotors.

After pre-processing the data, the FRESPID [15] utility from CIPHER was used to determine the frequency response of the system. Based on the obtained result, it



was possible to obtain the transfer function of the yaw movement using the NAVFIT [15] utility from CIFER. The transfer function is given in:

$$H_{yaw} = \frac{172130}{s^2 + 19.15s + 712.3} e^{-0.0288s}$$

This is a second order under damped system, with time delay equal to 29 ms. The principal cause of this time delay is the wireless communication through Bluetooth.

3.1.2. Identification using IDENT

A second approach for obtaining the transfer function of the yaw movement consisted in applying a PRBS (Pseudo Random Binary Signal) as input into the rudder channel of the helicopter. When generating a PRBS for system identification, it is important that it covers the whole frequency range for which the model should be valid. The amplitude of the input signal was switched between -0.2 and $+0.2$. The identification experiment consisted in generating an appropriate signal and injecting it into the process. The angular speed of the helicopter on the Z axis was recorded. Based on the input and the measured output it was possible to determine a transfer function using the System Identification toolbox (IDENT) from Matlab®. The obtained transfer function is shown in the following equation:

$$H_{yaw} = \frac{173273}{s^2 + 19.66s + 643.4} e^{-0.0087s}$$

This transfer function is similar to the one determined using CIFER, except for the time delay which is smaller than the sampling time (12 ms) in this case.

In order to choose which model characterizes best the yaw movement, the best fit index can be used as a criterion. The formula for computing the best fit index is:

$$\text{Best fit} = \left(1 - \frac{|y - \hat{y}|}{|y - \bar{y}|} \right) * 100$$

where y is the measured output, \hat{y} is the simulated output and \bar{y} is the mean value of the measured output. $|\cdot|$ is the Euclidian norm, which is defined for a vector (x_1, x_2, \dots, x_n) as:

$$|x_1, x_2, \dots, x_n| = \sqrt{\sum_{i=1}^n (x_i)^2}$$

The value of the best fit index applied for the transfer function determined using CIFER is 81.5652%, while the value of the best fit for the transfer function obtained from IDENT is 77.5230%. This shows that the model determined using CIFER describes better the system's dynamics. Although not significant, the 5%

improvement in the results using CIFER indicates that this model should be further used for control purposes.

3.1.3. Identification using Chirp-TFA

This method is based on the classical TFA (Transfer Function Analyzer) method which is able to find the frequency response of a system for one frequency point. The response of a linear system to a sinusoidal input is represented in Figure-10, whereas T is the signal period and Δt is the time shift:

$$\varphi = -\omega(t_1 - t_0) = -2\pi \frac{\Delta t}{T}$$

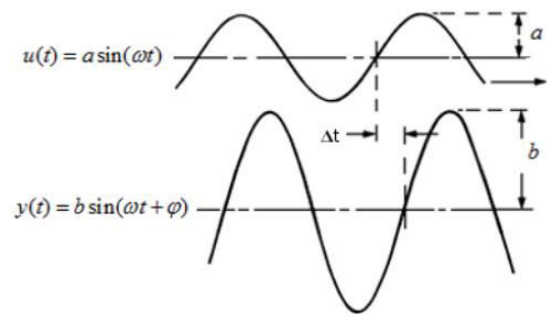


Figure-10. Sinusoidal input and output.

By sending into the process a sinusoidal input signal $u(t)$ and measuring the corresponding output signal $y(t)$ —ref. Figures 10 and 11—it is possible to find the magnitude $|G(j\omega)|$ and the phase shift $\angle G(j\omega)$ that characterizes the system for the ω (rad/s) frequency:

$$|G(j\omega)| = \frac{b}{a}$$

$$\angle G(j\omega) = \varphi$$

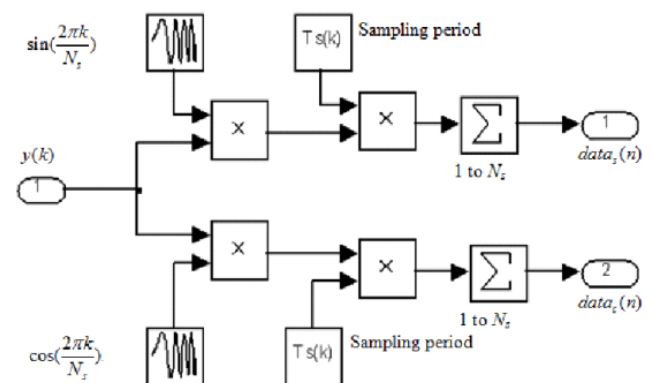


Figure-11. Algorithm implementation.

The output $y(t)$ is first multiplied by a sine and cosine of the test frequency ω . Then, the results of the multiplications are integrated over the period T_m :



$$\begin{aligned}
 y_s(T_m) &= \int_0^{T_m} y(t) \sin(\omega t) dt \\
 &= \int_0^{T_m} b \sin(\omega t + \varphi) \sin(\omega t) dt \\
 &\quad + \int_0^{T_m} n(t) \sin(\omega t) dt
 \end{aligned}$$

This equation becomes:

$$\begin{aligned}
 y_s(T_m) &= \frac{b}{2} T_m \cos(\varphi) - \frac{b}{2} \int_0^{T_m} \cos(2\omega t + \varphi) dt \\
 &\quad + \int_0^{T_m} n(t) \sin(\omega t) dt
 \end{aligned}$$

Analogously, for the cosine term it can be obtained:

$$\begin{aligned}
 y_c(T_m) &= \frac{b}{2} T_m \sin(\varphi) + \frac{b}{2} \int_0^{T_m} \sin(2\omega t + \varphi) dt \\
 &\quad + \int_0^{T_m} n(t) \cos(\omega t) dt
 \end{aligned}$$

If T_m is chosen as a multiple of the test frequency period than the second term in the previous equations then it goes to zero. If the integration time is long enough, and the noise has zero average, then the noise will be filtered. Thus it can be written:

$$y_s(T_m) \approx \frac{b}{2} \cos(\varphi)$$

$$y_c(T_m) \approx \frac{b}{2} \sin(\varphi)$$

from where it follows that:

$$b = \frac{2}{T_m} \sqrt{y_s^2(T_m) + y_c^2(T_m)}$$

$$\varphi = \tan^{-1} \left(\frac{y_c(T_m)}{y_s(T_m)} \right)$$

The revised TFA method (Chirp-TFA) proposes as input a sine sweep which is sampled at a varying rate. The novelty which is proposed by this method is that all the periods of the signal should have an equal number of samples. In order to achieve that, the input signal has to be sent into the system at variable sampling time and the system response has to be measured correspondingly. At every sampling instant, the sampling period is computed based on the value of the signal frequency at that moment. The frequency varies logarithmically between two predefined values which represent the frequency range of interest. The reason why the variable sampling is used is to obtain the same resolution in the frequency response, both for low and high frequencies. The algorithm for data processing after obtaining the experimental data is

presented in Figure-11, where $y(t)$ is the measured output signal and ω is the frequency of the signal (rad/s) at moment t and T_m is the total integration time which is chosen as an integer number of periods.

The form of the sine sweep signal is given by $\sin(2\pi f t) = \sin(2\pi f(t) k T(t))$. Hence, at every time instant t , a variable sampling period $T(t)$ is calculated, such that one period contains N samples. The relation is given by $f(t) T(t) = 1/N$. The N samples are then given by $\sin(2\pi k/N)$, with $k = 0, 1, \dots, N-1$. For example, at the n^{th} interval, it is obtained that:

$$data_s(n) = \sum_{k=N_s(N-1)}^{N_s N-1} y(k) \sin\left(\frac{2\pi k}{N}\right) T(k)$$

$$data_c(n) = \sum_{k=N_s(N-1)}^{N_s N-1} y(k) \cos\left(\frac{2\pi k}{N}\right) T(k)$$

where $T(k)$ represents the sampling period at the k^{th} sample in the data vector and

$$T(k) = \frac{1}{N_s f(k)}$$

where $f(k)$ denotes the frequency at the k^{th} sample. The linearly-varying instantaneous frequency at the time t can be found by using:

$$f(t) = f_0 + \frac{(f_1 - f_0)}{t_1} t$$

Considering that it is obtained one point in a Bode plot for each period on which it is integrated, it makes sense to increase the frequency exponentially with time, in order to get the same resolution (points per decade) for all frequency intervals in the plot. Therefore, the frequency points are calculated from:

$$\log[f(t)] = \log[f_0] + \frac{\log[f_1] - \log[f_0]}{t_1} t$$

Hence,

$$f(t) = f_0 \left(\frac{f_1}{f_0} \right)^{\frac{t}{t_1}}$$

which is then function of the design parameters. Notice that the sampling time is re-calculated in each sampling instant by an iterative algorithm; i.e. based on the desired number of samples in a period N_s , the frequency at each sampling instant from previous equation, the sampling period is given before and iterated until it does not change within the sampling instant. In practice, this is achieved within 2-3 iterations.



The result obtained for the yaw movement identification is presented in Figure-12 as a Bode diagram. The input sine sweep was defined for a frequency ranging from 1 Hz to 5 Hz and amplitude between ± 0.2 . The frequency-response obtained using Chirp-TFA matches the one obtained using CIFER. The only difference is the "noise" on the Chirp-TFA Bode plot, while the result from CIFER is smoother. This difference comes from different frequency resolution parameters used for the two methods. The transfer function for the Chirp-TFA method is the same as in CIFER method.

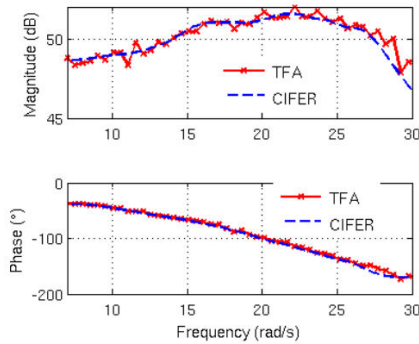


Figure-12. Bode diagrams comparison.

3.2 Control strategy

3.2.1. Controller design

The control system of a UAV can be split in three hierarchical layers: attitude control, trajectory control and mission control. The attitude control denotes the control at the lowest level and it directly regulates the actuators on the helicopter so that it achieves the desired attitude, respectively ϕ (roll), θ (pitch) and ψ (yaw) angles (recall here Figure-1). The yaw angle can be controlled with some degree of accuracy using the output of a gyroscope that measures the angular rate on the Z axis.

One way to control a UAV is to decompose the 4x4 MIMO system into 4 SISO systems and make the assumption that they are loosely coupled. In this case, this assumption is valid especially for the yaw movement which is not influenced by the other three (roll, pitch and altitude). Having this in mind, a controller has been designed based on knowledge of the transfer function.

The structure of the controller is presented in Figure-13. The inner closed loop regulates the angular rate based on the feedback received from the gyroscope on the Z axis. The proportional gain, integral gain and derivative gain of this PID controller were determined using FRtool [7], which is a graphical tool for controller design which allows the user to interactively modify the poles and zeros of the controllers. By using this tool, the time delay of the system does not have to be approximated (i.e. Padé) since it is represented as a shift in the phase.

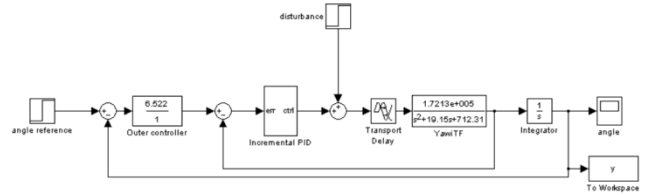


Figure-13. Simulink block scheme of the closed loop system.

In order to design the angular rate controller, some specifications were imposed: robustness 50%, settling time 0.6 s and overshoot 10% see Figure-14. The blue ellipse represents the imposed robustness and the red curve represents the overshoot and the settling time. In order for the closed loop system to meet the imposed specifications, the Nichols curve of the open loop system should not cross the two curves.

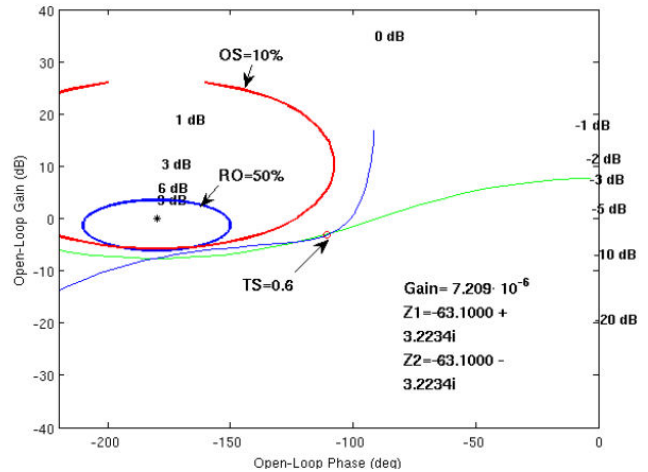


Figure-14. Nichols plot with closed loop specifications; PID design.

The formula of the obtained PID controller is:

$$H_c = \frac{7.209 \cdot 10^{-6} s^2 + 9.0990 \cdot 10^{-4} s + 0.02878}{s}$$

The standard form of the PID controller is:

$$H_c = K_p \left(1 + \frac{1}{T_i s} + T_d s \right) = \frac{K_p T_d s^2 + K_p s + K_p / T_i}{s}$$

Based on this, the parameters of the PID controller have been computed:

$$K_p = 9.0990 \cdot 10^{-4}; T_i = 0.0316; T_d = 0.0079$$

The outer loop controls the yaw angle of the helicopter, which can be approximated by integrating the measured angular rate. A simple software integrator was added to the system (see Figure-13). The yaw angle can be controlled using as feedback the angle computed by the



software integrator. Using FRtool, a P-controller for the yaw angle was obtained. The imposed specifications were: robustness $R_o = 50\%$, settling time $T_s = 1$ s and overshoot $OS = 20\%$.

The gain of the yaw angle controller is:

$$K_p = 6.522$$

The robustness imposed for the angular speed controller in the inner loop and for the angular position in the outer loop is $R_o = 50\%$. In order to test if the controllers meet this requirement, some simulations were performed to check how the controller would behave if the results obtained in the identification stage are not correct. In order to check that, the gain of the transfer function was increased by 50% in the first stage. In the second stage, the gain of the transfer function remained unchanged and the time delay was increased by 50%. The results of these simulations are presented in Figure-15. Both controllers are able to cope with the errors in the model. The performance of the controller diminishes, especially for an increase in the time delay, nevertheless it remains stable.

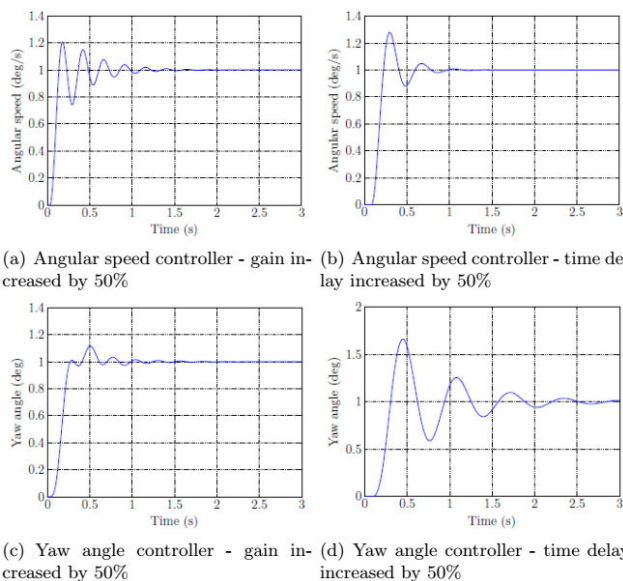


Figure-15. Robustness tests through simulation.

3.2.2. Digital control implementation

One way to implement a PID controller in a digital computer is by using an incremental form. The equations for this type of controller are presented below, where T_s is the sampling time, K_p is the gain, T_i is the integral time and T_d is the derivative time.

$$u(t) = u(t-1) + c_0 e(t) + c_1 e(t-1) + c_2 e(t-2)$$

where the coefficients are:

$$c_0 = K_p \left(1 + \frac{T_s}{T_i} + \frac{T_d}{T_s} \right)$$

$$c_1 = -K_p \left(1 + 2 \frac{T_d}{T_s} \right)$$

$$c_2 = K_p \frac{T_d}{T_s}$$

The controller was tested both for simulation and real life tests for two different situations: applying a disturbance and changing the reference angle during flight. In both situations the controller was able to perform the desired task and follow the specified angle. A comparison between the output of the simulated model and the measured yaw angle of the helicopter during flight is shown in Figure-16. In this experiment, the reference angle was changed between several values: 0° , 90° , -90° , 180° .

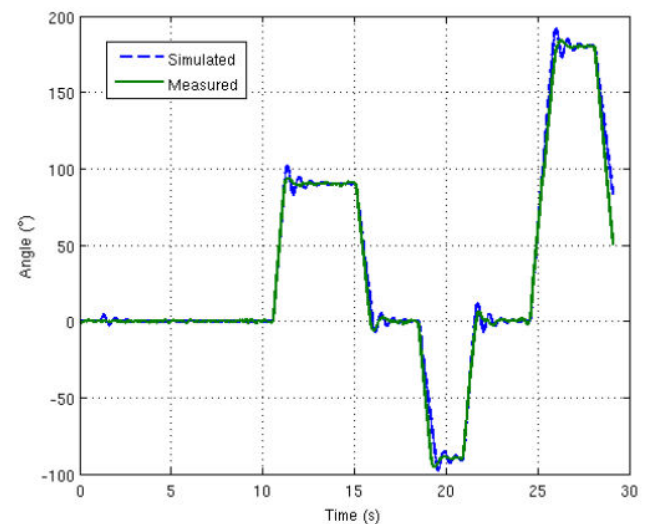


Figure-16. Controller test for reference change.

Overall, it can be concluded that the yaw control performed satisfactory; close to the desired specifications and that the simulation provides good agreement between model approximation and yaw dynamics.

4. CONCLUSIONS

This paper presented a simplified UAV structure which uses an IMU for determining the attitude of the aircraft. The communication with the controller implemented on a computer is done using Bluetooth communication and the commands are sent from the computer to the helicopter through a modified RC transmitter with the help of a PPM receiver.

After bringing the whole system in a functional state, modelling and identification of the yaw dynamics was performed. The yaw movement was chosen because it is weakly coupled with the other degrees-of-freedom. Another reason is that it is safer to put an identification signal on the rudder input than on aileron and elevator.

It was determined a model of the yaw movement, based on the physical principles, both mechanical and



electrical. The frequency response for the yaw movement was obtained using two methods: i) CIPHER and ii) a newly proposed Chirp-TFA method, providing similar results. This validates the newly developed identification technique.

The simulation results were validated with experimental data collected from the UAV during flight. The real life tests with the controller show that the helicopter has increased stability, allowing for a safer identification of the other movements.

The final goal of this project is to obtain a fully autonomous UAV based on the proposed architecture. The future stages are to obtain the transfer functions for pitch and roll so that a complete model of the helicopter is available. This will allow controlling the UAV based on the feedback from the sensors on all 3 degrees of freedom.

REFERENCES

- [1] W. Adiprawita, A. S. Ahmad and J. Semibiring. 2007. Automated flight test and system identification for rotary wing small aerial platform using frequency responses analysis. In: International Conference on Intelligent Unmanned Systems. pp. 50-56.
- [2] D. o. A. Aerial Robotics Group and M. I. o. T. Astronautics. 1999. The development of a small autonomous helicopter robot for search and rescue in hostile environments. In: Proceedings of the AUSSI Annual Symposium.
- [3] S. Bouabdallah, M. Becker and R. Siegwart. 2007. Autonomous miniature flying robots: coming soon! IEEE Robotics & Automation Magazine, September 2007: 88-98.
- [4] L. Chen and P. McKerrow. 2007. Modelling the Lama Coaxial Helicopter. In: Proceedings of the Australasian Conference on Robotics and Automation. University of Wollongong.
- [5] C. Ionescu, F. Robayo, R. D. Keyser and M. Naumovic. 2010. The frequency response analysis revisited. In: Proc. the IEEE 18th Mediterranean Conference on Control and Automation, number ISBN 978-1-4244-8090-6 in IEEE Cat Nr CFP10MED-CDR, pp. 1441-1446, Marrakesh, Morocco.
- [6] C. M. Ivler and M. B. Tischler. 2008. System identification modeling for flight control design. In: RAES Rotorcraft Handling-Qualities Conference. University of Liverpool.
- [7] R. D. Keyser and C. Ionescu. 2006. FRTool: A Frequency Response Tool for CACSD in Matlab. Proceedings of the 2006 IEEE Conference on Computer Aided Control Systems Design. pp. 2275-2280.
- [8] B. Kim, Y. Chang, and M. H. Lee. 2006. System identification and 6-dof hovering controller design of unmanned model helicopter. JSME International Journal. 49: 1048-1057.
- [9] H. J. Kim and D. H. Shim. 2003. A flight control system for aerial robots: algorithms and experiments. Control Engineering Practice. 11:1389-1400.
- [10] B. Mettler, M. Tischler and T. Kanade. 2000. System identification of a model-scale helicopter. Technical report, Carnegie Mellon University.
- [11] B. Mettler, M. B. Tischler, and T. Kanade. 1999. System Identification of Small-Size Unmanned Helicopter Dynamics. In American Helicopter Society 55th Forum.
- [12] J. Meyer, F. de Plessis, and W. Clarke. 2009. Design considerations for long endurance unmanned aerial vehicles. Aerial Vehicles. pp. 443-497.
- [13] S. M. Miller, R. B. MacCurdy, W. R. Kidd and J. M. Hudson. 2008. Stabilization and control of a micro-scale helicopter.
- [14] D. Schaafroth, C. Bermes, S. Bouabdallah and R. Siegwart. 2009. Modeling and system identification of the mufly micro helicopter. Journal of Intelligent and Robotic Systems.
- [15] M. B. Tischler. CIPHER User's Guide Student Version 5.2.00. US Army ATCOM, Ames Research Center, Moffett Field, California, USA.
- [16] M. B. Tischler and R. K. Remple. 2006. Aircraft and rotorcraft system identification. American Institute of Aeronautics and Astronautics.